

## Supporting Information

### Dual luminescent covalent organic framework for nitro-explosives detection

Muhammad Faheem,<sup>a</sup> Saba Aziz,<sup>a</sup> Xiaofei Jing,<sup>a</sup> Tingting Ma,<sup>a</sup> Junyi Du,\*<sup>b</sup> Fuxing Sun,<sup>c</sup> Yuyang Tian\*<sup>a</sup> and Guangzhan Zhu<sup>a</sup>

<sup>a</sup> Key Laboratory of Polyoxometalate Science of Ministry of Education, Northeast Normal University, Changchun, 130024, P. R. China. E-mail: [tianyy100@nenu.edu.cn](mailto:tianyy100@nenu.edu.cn)

<sup>b</sup> School of Material Science and Engineering, Beijing Institute of Technology, Beijing 100081, P. R. China, E-mail: [junyi\\_du@bit.edu.cn](mailto:junyi_du@bit.edu.cn)

<sup>c</sup> State Key Laboratory of Inorganic Synthesis and Preparative Chemistry, College of Chemistry, Jilin University, Changchun 130012, P. R. China.

## Table of Contents

<b>Section</b>	<b>Detail</b>	<b>Page No.</b>
i	<sup>13</sup> C CP/MAS Solid-state NMR spectrum of DL-COF	S3
ii	PXRD pattern of DL-COF with simulated AA and AB-stacking structures	S4
iii	Pore size of simulated AA-stacking structure	S5
iv	Simulated structures AA-stacking on base of ETTA orientation	S6
v	Pawley refined simulation patterns of DL-COF	S7
vi	Thermal stability test (TGA, DSC)	S8
vii	Chemical stability test XRD and FT-IR analysis	S9
viii	UV-Visible absorbance of DL-COF and tested nitro explosives analytes	S10
ix	XPS measurements of DL-COF and 4-NP+DL-COF	S11
x	Limit of detection (LOD) calculations of nitro explosives analytes	S12-S16
xi	Quenching efficiency (%) against concentrations of nitro explosives analytes	S17
xii	Fluorescence quenching pattern of non-explosives analytes	S18
xiii	Comparison study of tested nitro explosives analytes with COFs and MOFs	S19-S23
xiv	TCSPC calculation for average fluorescence lifetime measurement	S24
xv	References	S25

(i)  **$^{13}\text{C}$  CP/MAS Solid-state NMR spectrum of DL-COF**

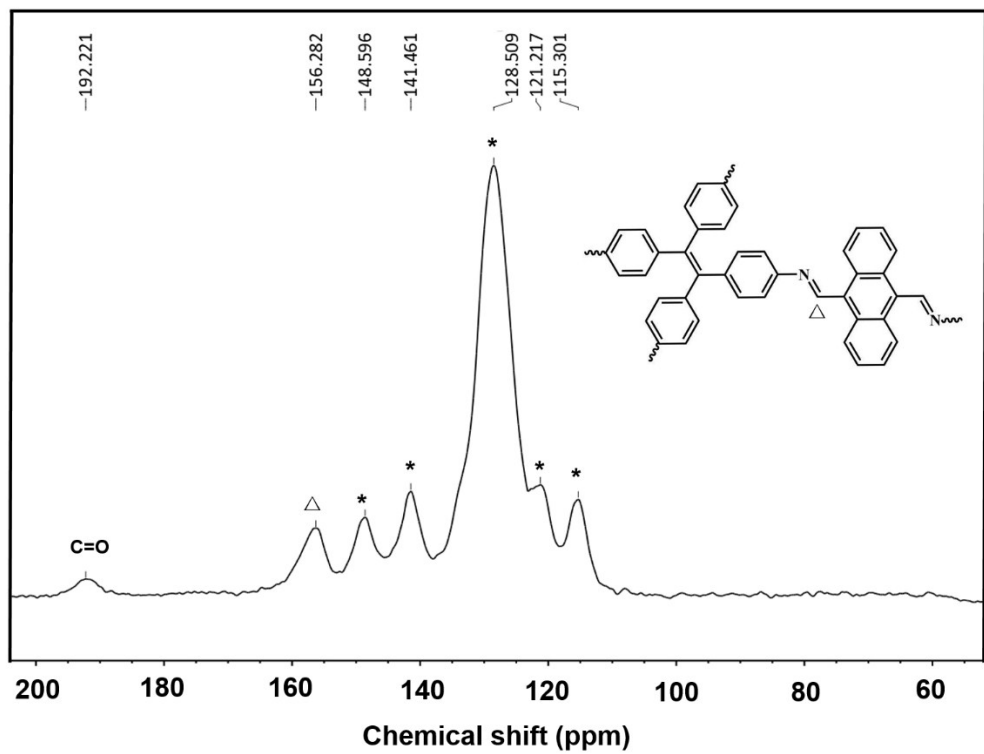


**Fig. S1**  $^{13}\text{C}$  CP/MAS Solid-state NMR spectrum of DL-COF: The triangle ( $\triangle$ ) represent chemical shift of imine carbon and the asterisks (\*) represent chemical shifts of aromatic carbons.

**(ii) PXRD pattern of DL-COF with simulated AA and AB-stacking structures**

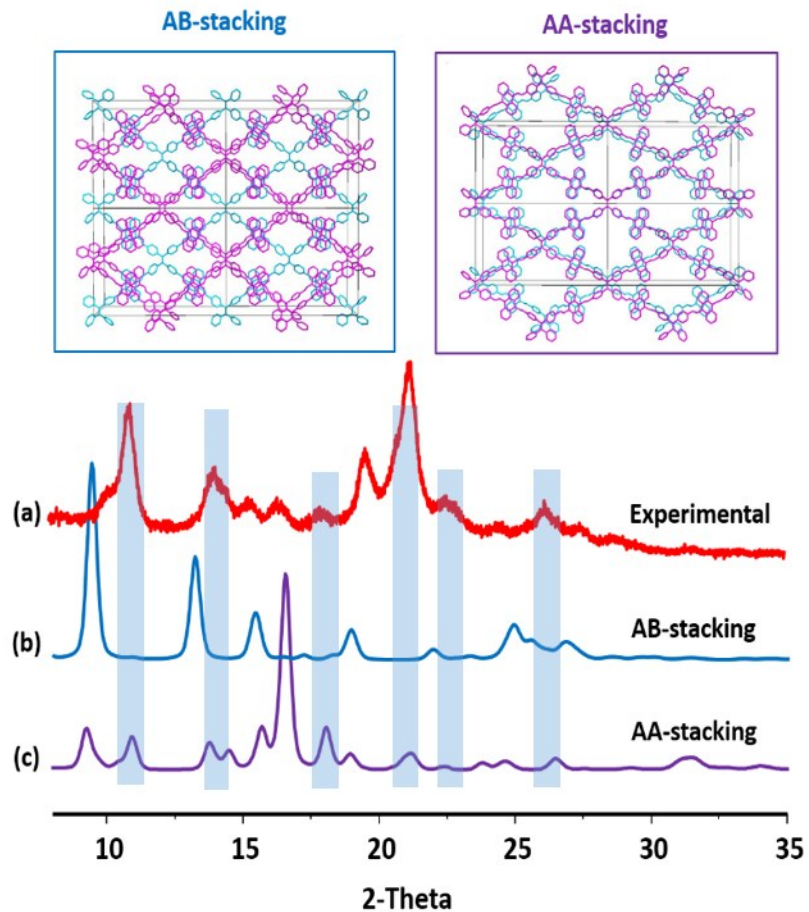


**Fig. S2** (a) Experimentally observed PXRD pattern of DL-COF, (b) Simulated PXRD pattern for AB-stacking structure and (c) Simulated PXRD pattern for AA-stacking structure.

**(iii) Pore size of simulated AA-stacking structure**

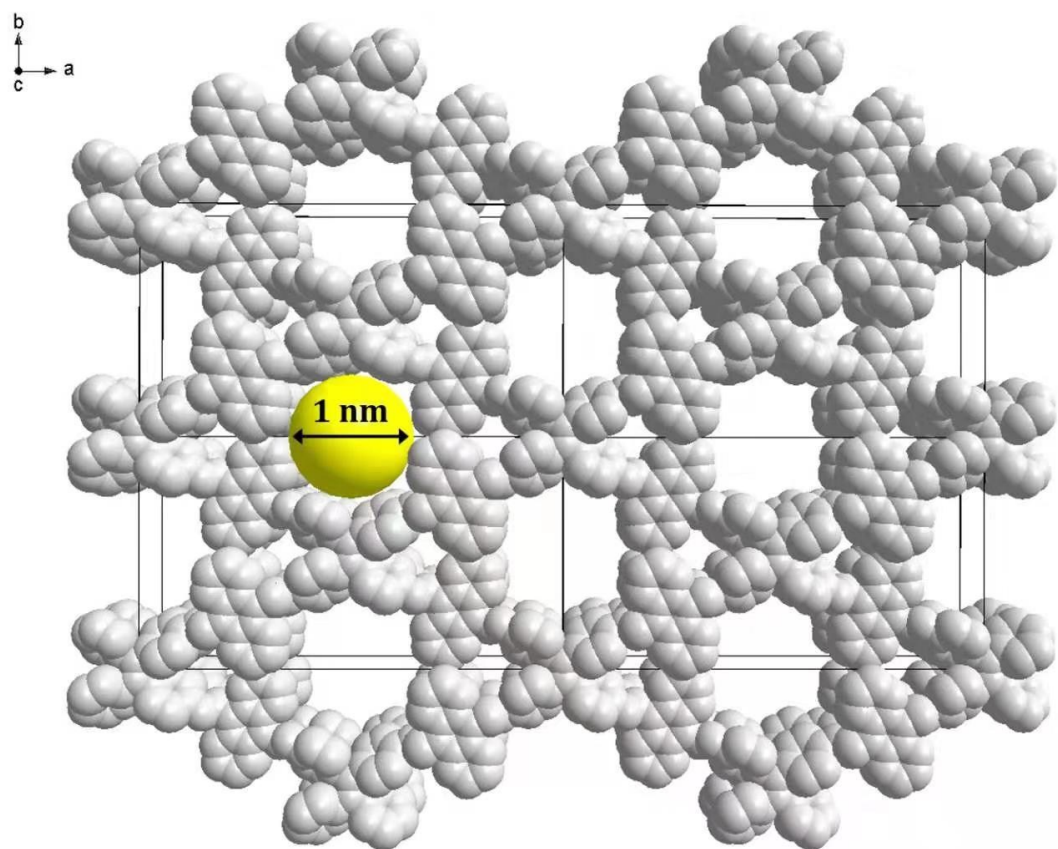


**Fig. S3** Pore size of simulated AA-stacking structure

**(iv) Simulated structures of AA-stacking on base of ETTA orientation**

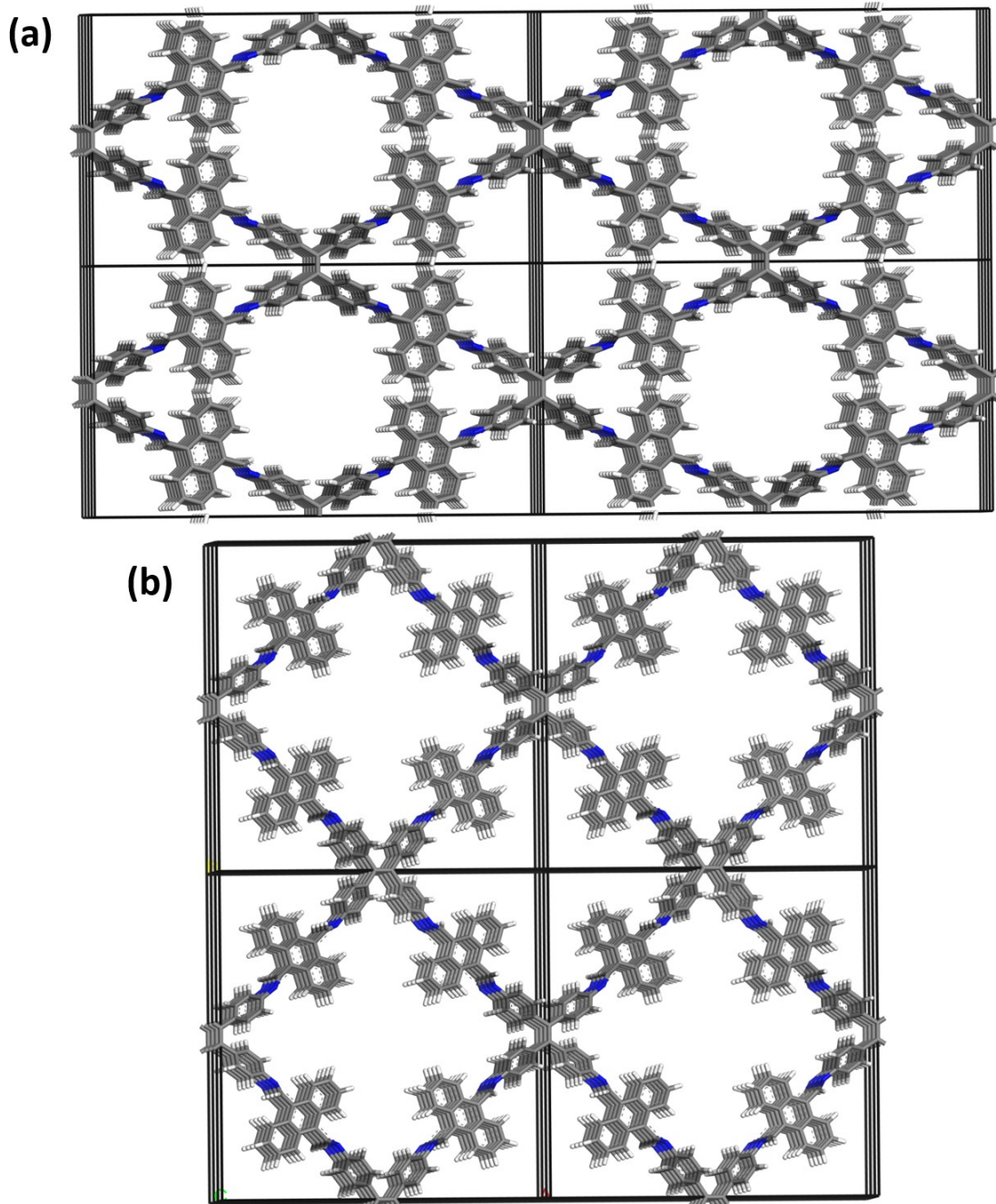


**Fig. S4** Simulated AA-stacking structures on base of ETTA orientation

(iv) Pawley refined simulation patterns of DL-COF

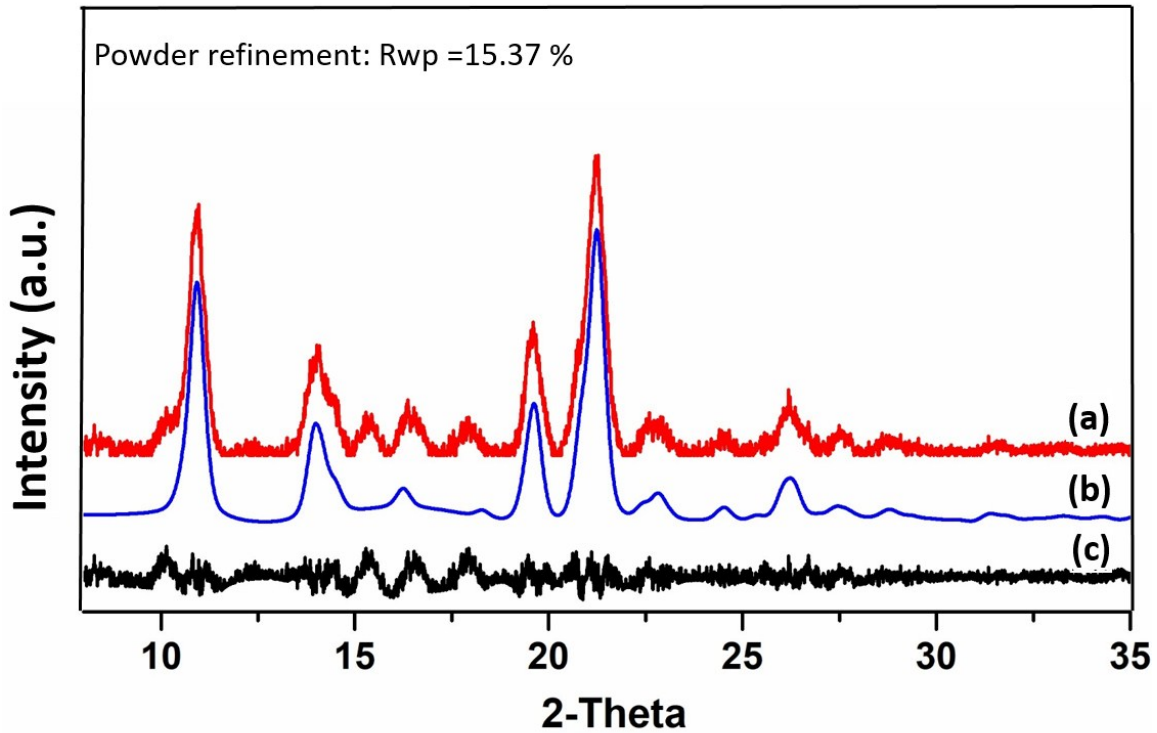


**Fig. S5** XRD patterns of the DL-COF: (a) experimental, (b) Pawley refined and (c) difference between experimental and calculated data.

(vi) Thermal stability test of DL-COF

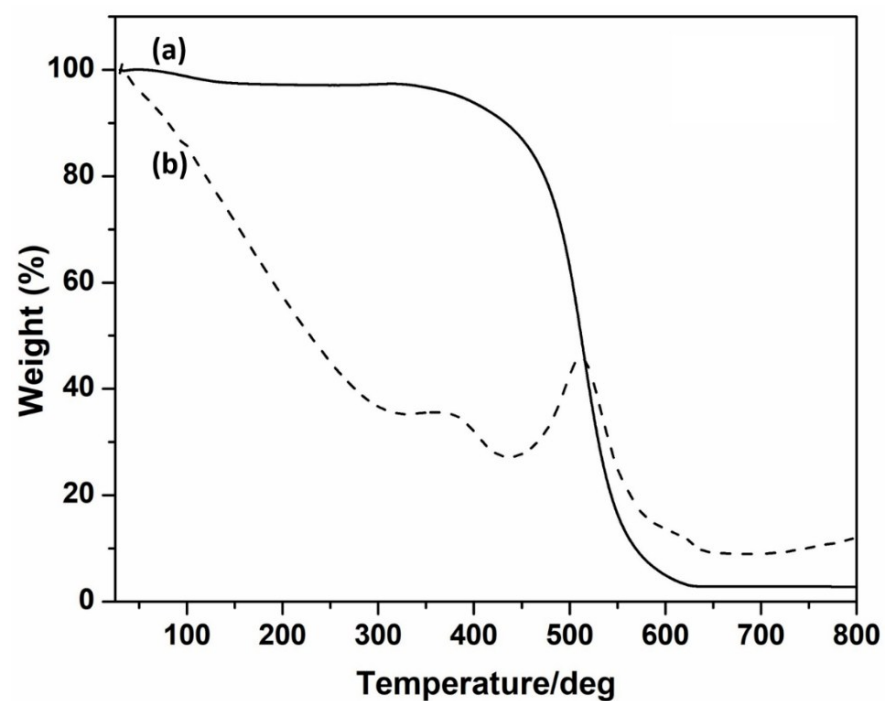
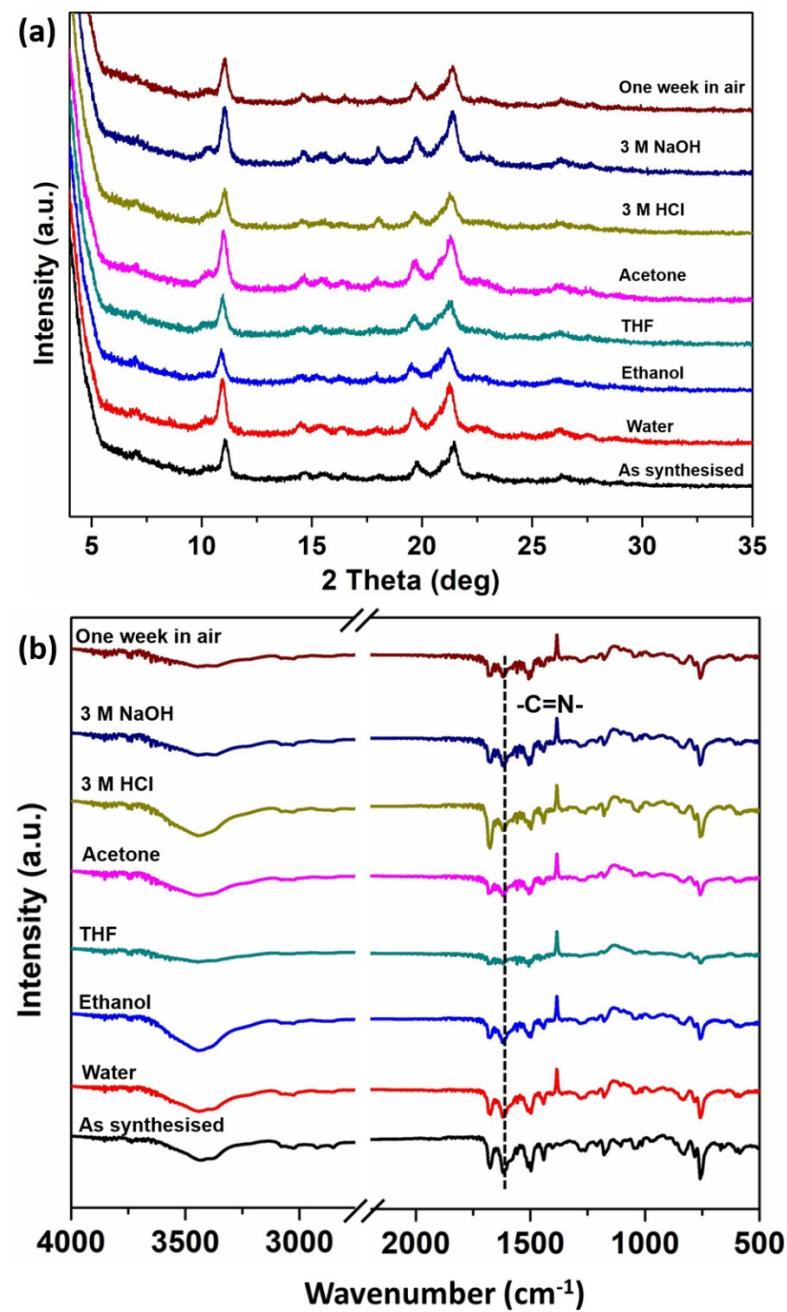


Fig. S6 (a) TGA and (b) DSC curves of the DL-COF

(vii) Chemical stability tests of DL-COF



**Fig. S7** (a) PXRD patterns of the DL-COF after treatment in different chemical environments (b) FTIR spectra of the DL-COF after treatment in different chemical environments.

(viii) UV-Visible absorbance of DL-COF and tested nitro explosive analytes

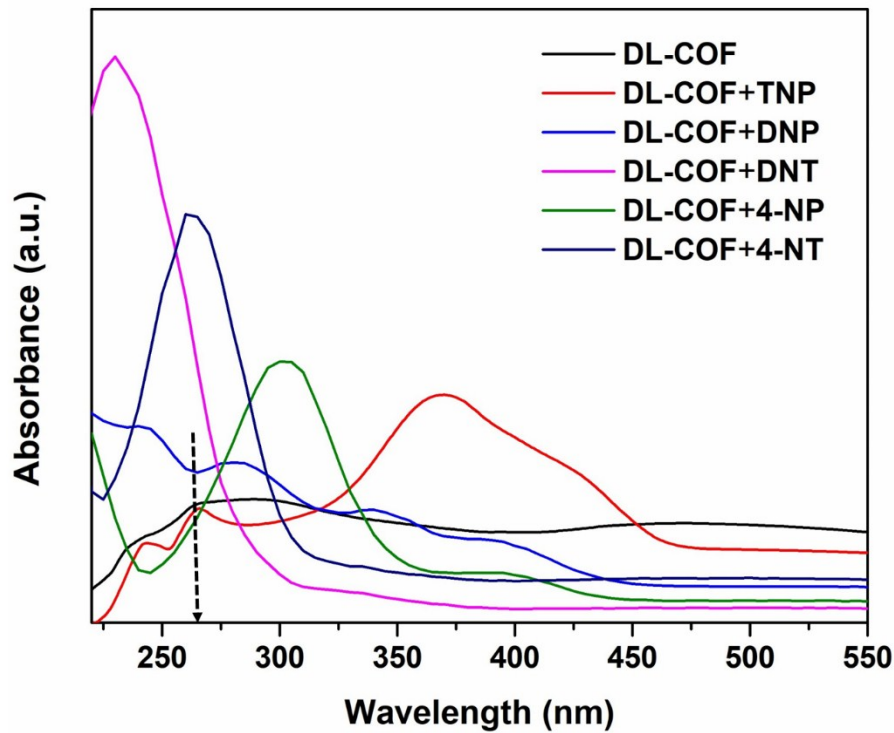


**Fig. S8** UV-visible absorbance of DL-COF and DL-COF with nitro explosive analytes.

(ix) XPS measurements of DL-COF and 4-NP+DL-COF

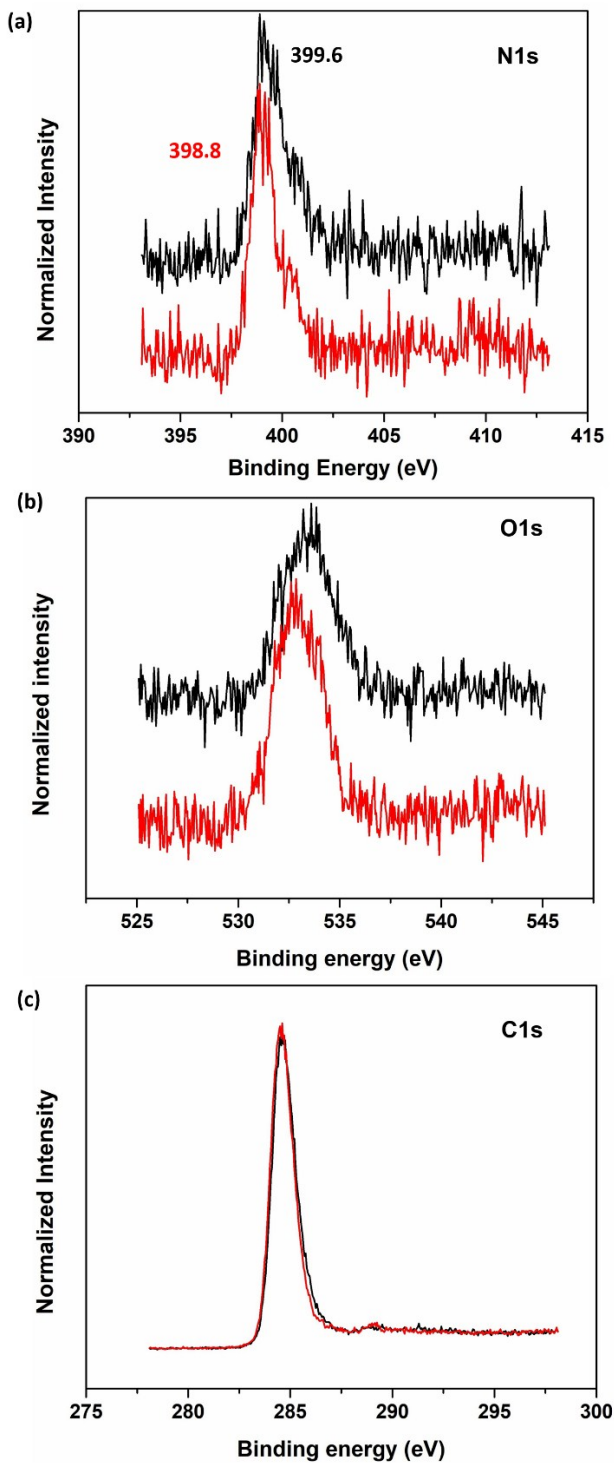


**Fig. S9** XPS spectra of DL-COF (black curves) and 4-NP+DL-COF (red curves). The C 1s signal at 284.5 eV, which is attributed to aromatic carbons. The O 1s at a binding energy of 533 eV and 532 eV are due to air contamination, water and hydroxyl groups in the sample. [21]

**(x) Limit of detection (LOD) calculations of nitro explosive analytes**

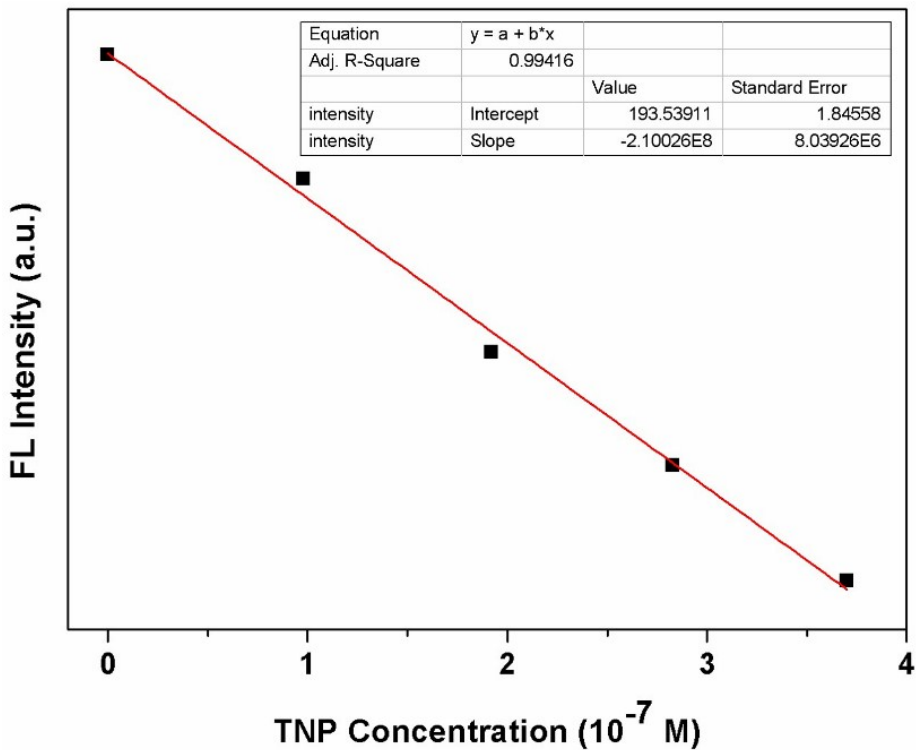


**Fig. S10** Linear region of fluorescence intensity of DL-COF upon incremental addition of TNP at  $\lambda_{em} = 311$  nm (upon  $\lambda_{ex} = 264$  nm) at room temperature.

**Calculation of Detection limit (LOD) for TNP:**

Slope from graph (m)	2.10026E+8 M <sup>-1</sup>
Standard deviation ( $\sigma$ )	4.0124
Limit of detection ( $3\sigma/m$ )	57.31 nM ( <b>13.10 ppb</b> )

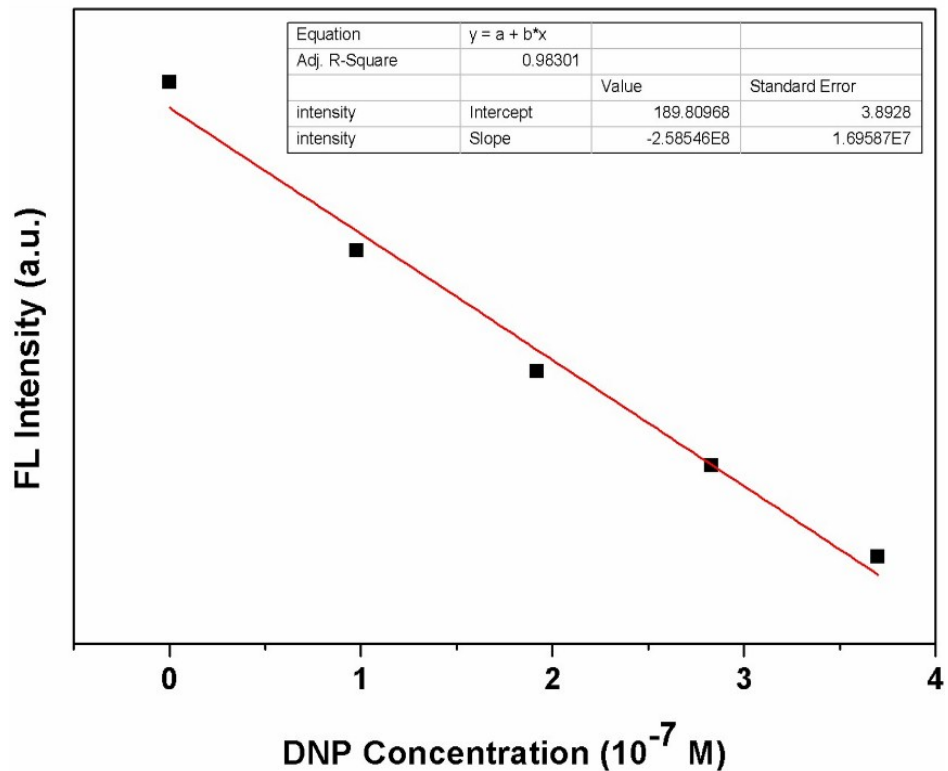


**Fig. S11** Linear region of fluorescence intensity of DL-COF upon incremental addition of DNP at  $\lambda_{em} = 311$  nm (upon  $\lambda_{ex} = 264$  nm) at room temperature.

**Calculation of Detection limit (LOD) for DNP:**

Slope from graph (m)	$2.58546E+8 \text{ M}^{-1}$
Standard deviation ( $\sigma$ )	4.0124
Limit of detection ( $3\sigma/m$ )	46.50 nM ( <b>8.56 ppb</b> )

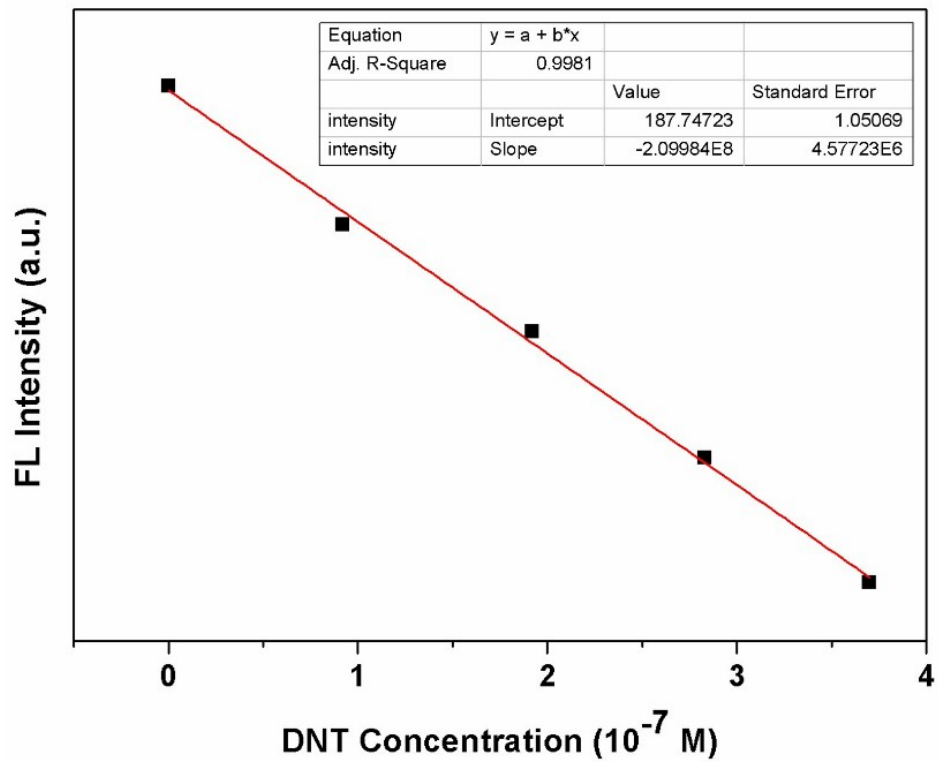


**Fig. S12** Linear region of fluorescence intensity of DL-COF upon incremental addition of DNT at  $\lambda_{em} = 311$  nm (upon  $\lambda_{ex} = 264$  nm) at room temperature.

**Calculation of Detection limit (LOD) for DNT:**

Slope from graph (m)	2.09984E+8 M <sup>-1</sup>
Standard deviation ( $\sigma$ )	4.0124
Limit of detection ( $3\sigma/m$ )	57.32 nM ( <b>10.40 ppb</b> )

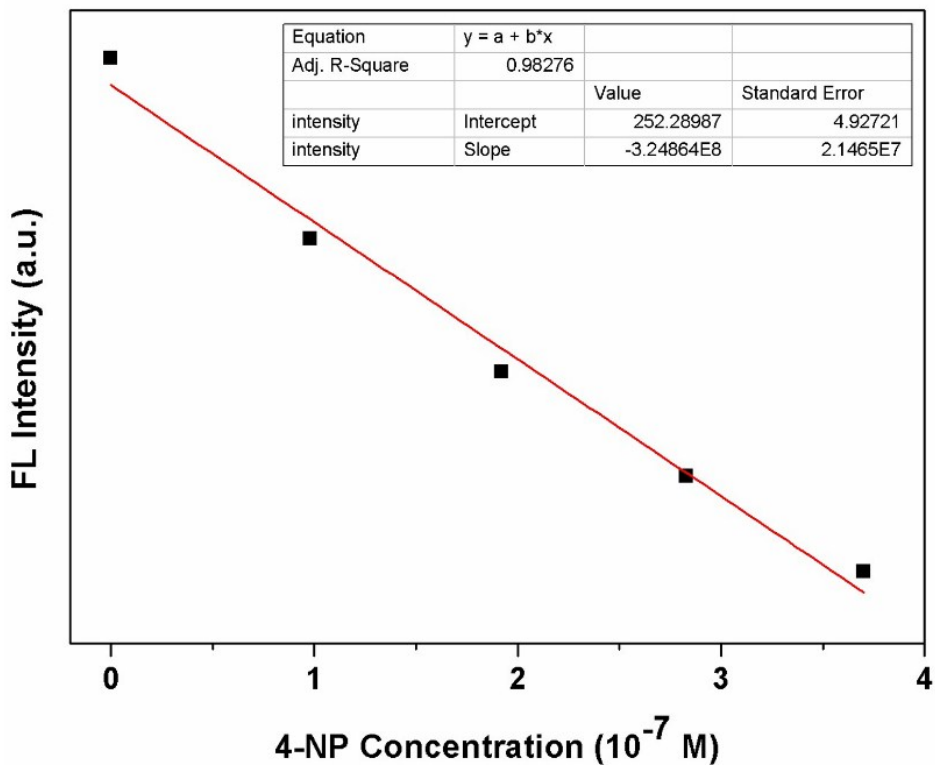


**Fig. S13** Linear region of fluorescence intensity of DL-COF upon incremental addition of 4-NP at  $\lambda_{em} = 311$  nm (upon  $\lambda_{ex} = 264$  nm) at room temperature.

**Calculation of Detection limit (LOD) for 4-NP:**

Slope from graph (m)	3.24864E+8 M <sup>-1</sup>
Standard deviation ( $\sigma$ )	4.0124
Limit of detection ( $3\sigma/m$ )	37.05 nM ( <b>5.15 ppb</b> )

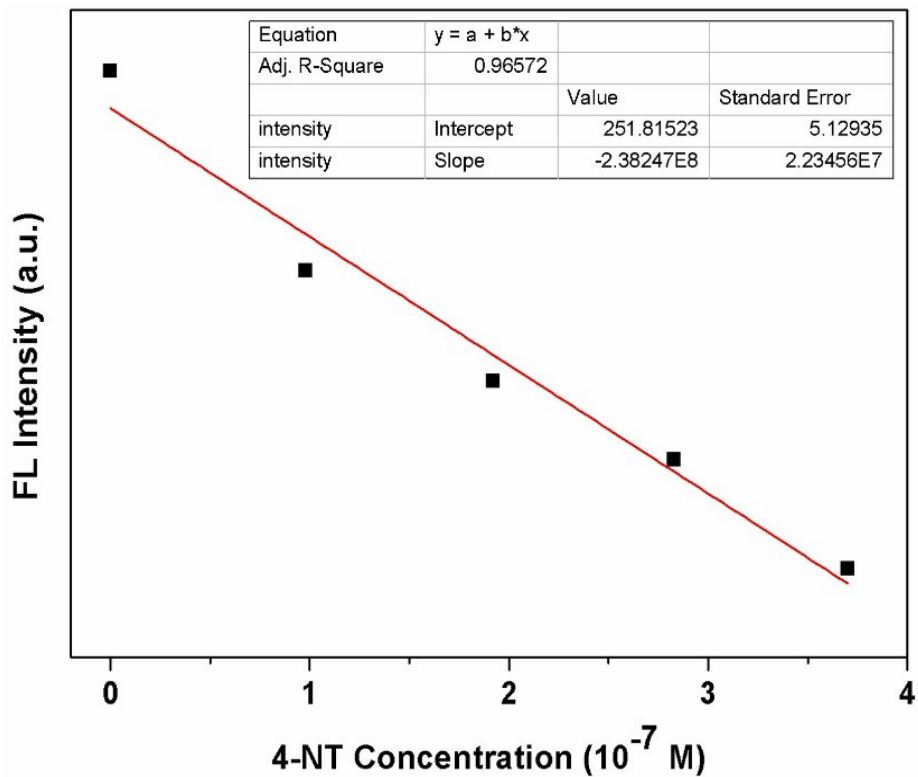


**Fig. S14** Linear region of fluorescence intensity of DL-COF upon incremental addition of 4-NT at  $\lambda_{em} = 311$  nm (upon  $\lambda_{ex} = 264$  nm) at room temperature.

**Calculation of Detection limit (LOD) for 4-NT:**

Slope from graph (m)	2.38247E+8 M <sup>-1</sup>
Standard deviation ( $\sigma$ )	4.0124
Limit of detection ( $3\sigma/m$ )	50.52 nM ( <b>6.92 ppb</b> )

(xi) Quenching efficiency (%) against concentrations of nitro explosive analytes

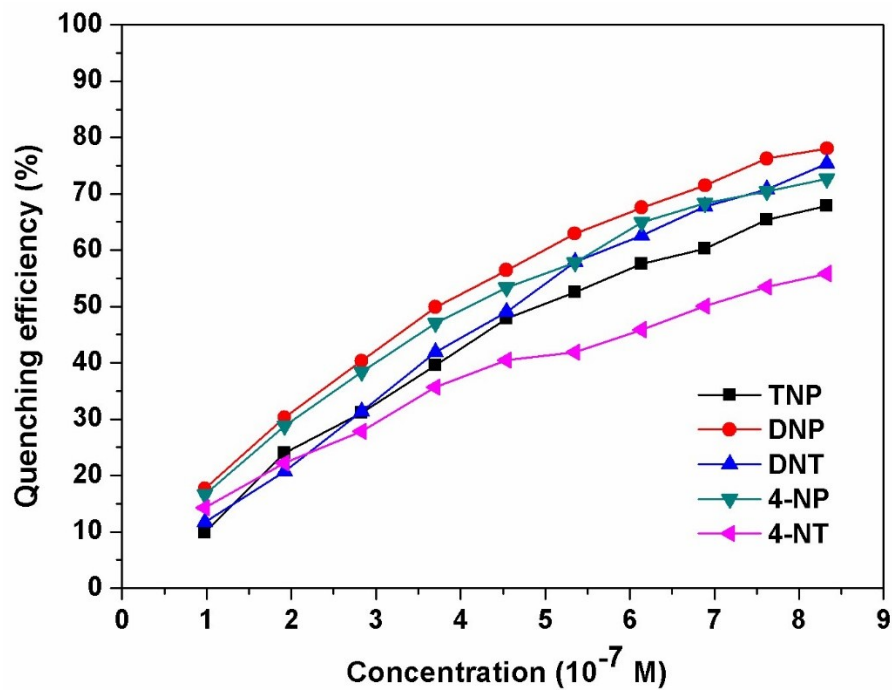


**Fig. S15** Quenching efficiency (%) against various concentrations of nitro explosive analytes.

(xii) Fluorescence quenching pattern of non-explosives analytes

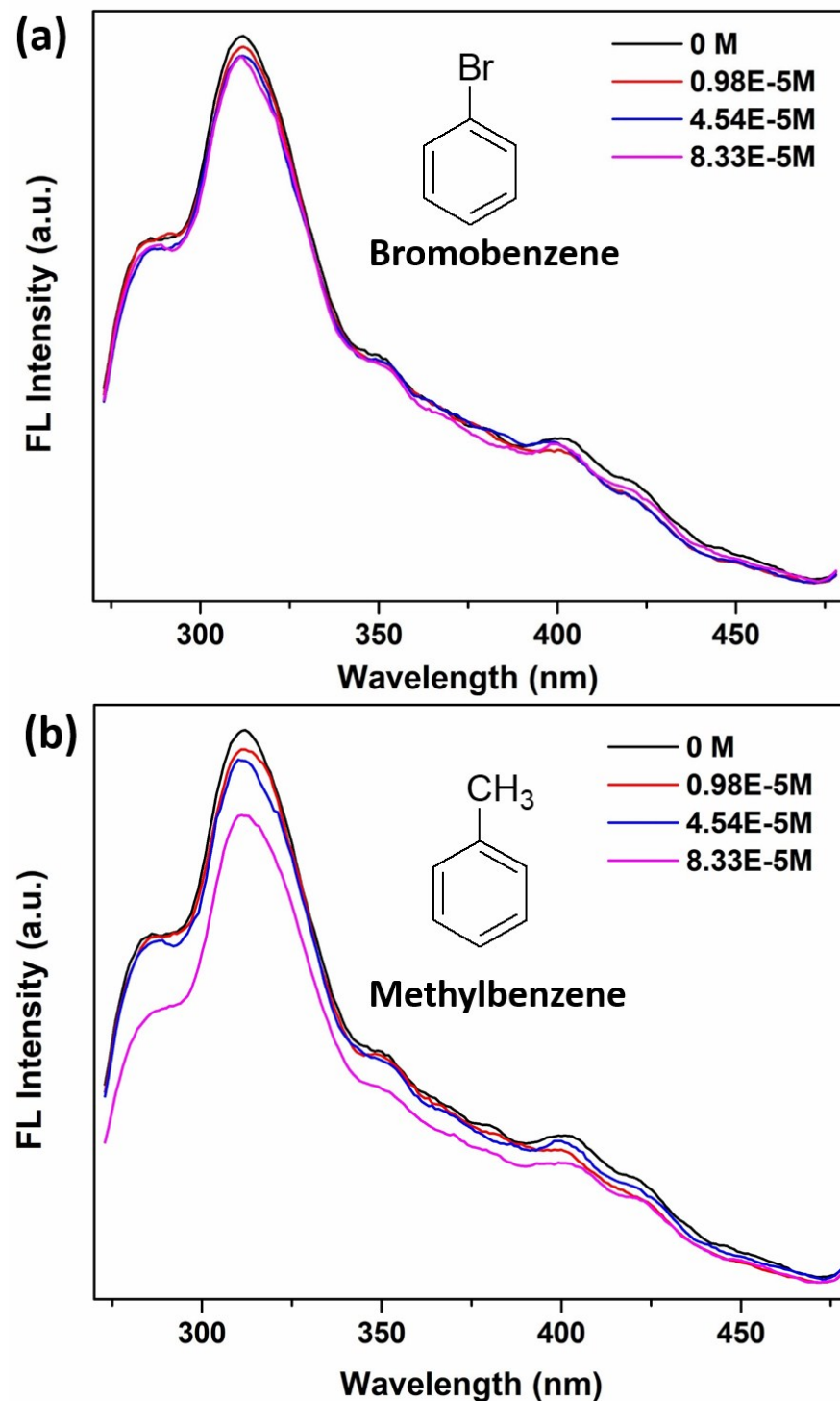


**Fig. S16** Fluorescence quenching pattern of non-explosives analytes at  $\lambda_{em} = 311$  nm (upon  $\lambda_{ex} = 264$  nm) at room temperature.

**(xiii) Comparison study of tested nitro explosive analytes with reported COFs and MOFs**

**Table S1.** Comparison study of TNP with other COFs and MOFs.

Materials	Ksv ( $M^{-1}$ )	LOD	Medium	Ref.
DL-COF	$2.42 \times 10^6$	$57.31 \times 10^{-9} M$ (13.10 ppb)	EtOH	This work
Covalent organic frameworks (COFs)				
TAPB-TFP-COF	$3.20 \times 10^4$	NA	MeCN	[1]
iPrTAPB-TFPB-COF	$3.0 \times 10^4$	NA	MeCN	[1]
iPrTAPB-TFP-COF	$1.8 \times 10^4$	NA	MeCN	[1]
Metal organic frameworks (MOFs)				
$[(CH_3)_2NH_2].2[Eu_6(OH)_8(ADBA)_6(H_2O)_6]$ (DMF) <sub>15</sub>	$1.282 \times 10^5$	NA	D. Water	[2]
$\{[Zn(C_{34}H_{18}O_8)_{0.5}(C_{20}N_2H_{16})_{0.5}].[0.5(C_{20}N_2H_{16})]\}_n$	$8.10 \times 10^4$	NA	DMF	[3]
$\{[0.2Me_2NH_2][Zn_8(ad)_4(BPDC)_6] \cdot G\}_n$	$6.40 \times 10^4$	$12.90 \times 10^{-6} M$	Water	[4]
$[Cd(NDC)_{0.5}(PCA)]_n$	$3.50 \times 10^4$	NA	MeCN	[5]
$[Zn_2(NDC)_2(bpy)].Gx$	$0.40 \times 10^4$	NA	EtOH	[6]

NA= Not available

**Table S2.** Comparison study of DNP with other COFs and MOFs.

Materials	K <sub>sv</sub> (M <sup>-1</sup> )	LOD	Medium	Ref.
DL-COF	4.28 ×10 <sup>6</sup>	46.50×10 <sup>-9</sup> M (8.56 ppb)	EtOH	This work
Covalent organic frameworks (COFs)				
TRIPTA-COF	2.13×10 <sup>6</sup>	NA	MeCN	[7]
TfpBDH-COF	3.5×10 <sup>3</sup>	NA	Isopropylalcohol	[8]
Py-Azine COF	2.10×10 <sup>3</sup>	NA	MeCN	[9]
Metal organic frameworks (MOFs)				
In-ADBA	8.99×10 <sup>4</sup>	NA	Water	[2]
FJI-H15	2.54×10 <sup>4</sup>	NA	Dimethylacetamide	[10]
UiO-68-mtpdc/etpdc	2.30×10 <sup>4</sup>	NA	Methanol	[11]

NA= Not available

**Table S3.** Comparison study of DNT with other COFs and MOFs.

Materials	K <sub>sv</sub> (M <sup>-1</sup> )	LOD	Medium	Ref.
DL-COF	3.71 ×10 <sup>6</sup>	57.32×10 <sup>-9</sup> M (10.40 ppb)	EtOH	This work
Covalent organic frameworks (COFs)				
TRIPTA-COF	1.19×10 <sup>6</sup>	NA	MeCN	[7]
Py-Azine COF	9.10×10 <sup>3</sup>	NA	MeCN	[9]
iPrTAPB-TFP-COF	8.80×10 <sup>3</sup>	NA	MeCN	[1]
TAPB-TFP-COF	8.70×10 <sup>3</sup>	NA	MeCN	[1]
iPrTAPB-TFPB-COF	1.20×10 <sup>3</sup>	NA	MeCN	[1]
Metal organic frameworks (MOFs)				
[Y <sub>1.8</sub> Eu <sub>0.2</sub> (PDA) <sub>3</sub> (H <sub>2</sub> O)1]·2H <sub>2</sub>	5.01×10 <sup>4</sup>	NA	MeCN	[12]
[Zn <sub>2</sub> (NDC) <sub>2</sub> (bpy)]·Gx	5.1×10 <sup>3</sup>	NA	EtOH	[13]
Eu <sub>3</sub> (MFDA) <sub>4</sub> (NO <sub>3</sub> ) <sub>3</sub> (DMF) <sub>3</sub>	1.30×10 <sup>3</sup>	NA	DMF	[14]

NA= Not available

**Table S4.** Comparison study of 4-NP with other COFs and MOFs.

Materials	K <sub>sv</sub> (M <sup>-1</sup> )	LOD	Medium	Ref.
DL-COF	3.18 ×10 <sup>6</sup>	37.05×10 <sup>-9</sup> M (5.15 ppb)	EtOH	This work
Covalent organic frameworks (COFs)				
TRIPTA-COF	5.80×10 <sup>5</sup>	NA	MeCN	[7]
Py-Azine COF	5.90×10 <sup>2</sup>	NA	MeCN	[9]
Metal organic frameworks (MOFs)				
UPC-21	3.09 ×10 <sup>6</sup>	0.0896 ppm	DMSO	[15]
In-ADBA	5.11 ×10 <sup>4</sup>	NA	Water	[2]
BUT-13	4.70 ×10 <sup>4</sup>	NA	Water	[16]
BUT-12	4.20 ×10 <sup>4</sup>	NA	Water	[16]
[Zn <sub>2</sub> (TPOM)(NH <sub>2</sub> -BDC) <sub>2</sub> ]·4H <sub>2</sub> O	2.17 ×10 <sup>4</sup>	NA	DMF	[17]
UPC-17	1.26 ×10 <sup>4</sup>	NA	THF	[18]
[Zn(L)(H <sub>2</sub> O)]·H <sub>2</sub> O	1.25 ×10 <sup>4</sup>	3.34 μM	Water	[19]
UiO-68-mtpdc/etpdc	7.20 ×10 <sup>3</sup>	NA	Methanol	[11]

NA= Not available

**Table S5.** Comparison study of 4-NT with other COFs and MOFs.

Materials	K <sub>sv</sub> (M <sup>-1</sup> )	LOD	Medium	Ref.
DL-COF	1.56 ×10 <sup>6</sup>	50.52×10 <sup>-9</sup> M (6.92 ppb)	EtOH	This work
Covalent organic frameworks (COFs)				
Py-Azine COF	4.5 ×10 <sup>2</sup>	NA	MeCN	[9]
Metal organic frameworks (MOFs)				
[Y <sub>1.8</sub> Eu <sub>0.2</sub> (PDA) <sub>3</sub> (H <sub>2</sub> O)1]·2H <sub>2</sub> O	1.1×10 <sup>4</sup>	NA	MeCN	[12]
[Zn <sub>2</sub> (NDC) <sub>2</sub> (bpy)]·Gx	1.16×10 <sup>4</sup>	NA	EtOH	[13]
[Tb0.2Y0.18(PDA)3(H <sub>2</sub> O)1]·2H <sub>2</sub> O	0.39×10 <sup>4</sup>	NA	MeCN	[20]

**(xiv) TCSPC calculation for average fluorescence lifetime measurement**

**Table S6.** TCSPC calculation of DL-COF and nitro explosives analytes

Sample	T1	T2	B1	B2	A1=[B1/SumB]	A2=[B2/SumB]	$\langle I \rangle$ (ns)	$\chi^2$
DL-COF	1.3413	12.1924	0.106	0.015	0.8760	0.1239	2.68	1.18
DL-COF+TNP	1.4514	6.5424	0.077	0.020	0.7938	0.2061	2.50	1.47
DL-COF+DNP	1.0415	7.9345	0.120	0.012	0.9090	0.0909	1.66	0.94
DL-COF+DNT	0.9924	7.0937	0.111	0.015	0.8809	0.1190	1.71	0.93
DL-COF+4-NP	1.4020	6.3395	0.084	0.013	0.8659	0.1340	2.06	0.92
DL-COF+4-NT	1.2320	7.5945	0.090	0.015	0.8571	0.1428	2.14	1.07

Where,  $\langle I \rangle = A1T1+A2T2$  and  $\chi^2$  is the accuracy factor. [7]

## (xv) References

1. D. Kaleeswaran, P. Vishnoi, and R. Murugavel, *J. Mater. Chem. C*, 2015, **3**, 7159–7171.
2. X. Liu, B. Liu, G. Li, and Y. Liu, *J. Mater. Chem. A*, 2018, **6**, 17177–17185.
3. B. Wang, X. L. Lv, D. Feng, L. H. Xie, J. Zhang, M. Li, Y. Xie, J. R. Li, and H. C. Zhou, *J. Am. Chem. Soc.*, 2016, **138**, 6204–6216.
4. B. Joarder, A. V. Desai, P. Samanta, S. Mukherjee, and S. K. Ghosh, *Chem. Eur. J.*, 2015, **21**, 965–969.
5. S. S. Nagarkar, B. Joarder, A. K. Chaudhari, S. Mukherjee, and S. K. Ghosh, *Angew. Chem. Int. Ed.* 2013, **52**, 2881–2885.
6. K. S. Asha, A. Bhattacharyya, and S. Mandal, *J. Mater. Chem. C*, 2014, **2**, 10073–10081.
7. R. Gomes, and A. Bhumik, *RSC Adv.*, 2016, **6**, 28047–28054.
8. G. Das, B. P. Biswal, S. Kandambeth, V. Venkatesh, G. Kaur, M. Addicoat, T. Heine, S. Verma, and R. Banerjee, *Chem. Sci.*, 2015, **6**, 3931–3939.
9. S. Dalapati, S. Jin, J. Gao, Y. Xu, A. Nagai, and D. Jiang, *J. Am. Chem. Soc.*, 2013, **135**, 17310–17313.
10. H. Xue, D. Song, C. Liu, G. Lyu, D. Yuan, F. Jiang, Q. Chen, and M. Hong, *Chem. Eur. J.*, 2018, **24**, 11033–11041.
11. Q. Y. Li, Z. Ma, W. Q. Zhang, J. L. Xu, W. Wei, H. Lu, X. Zhao, and X. J. Wang, *Chem. Commun.*, 2016, **52**, 11284–11287.
12. D. K. Singha, P. Majee, S. K. Mondal, and P. Mahata, *Eur. J. Inorg. Chem.*, 2015, 1390–1397.
13. K. S. Asha, K. Bhattacharyya, and S. Mandal, *J. Mater. Chem. C*, 2014, **2**, 10073–10081.
14. X. Zhou, H. Li, H. Xiao, L. Li, Q. Zhao, T. Yang, J. Zuo, and W. Huang, *Dalton Trans.*, 2013, **42**, 5718–5723.
15. M. Zhang, L. Zhang, Z. Xiao, Q. Zhang, R. Wang, F. Dai, and D. Sun, *Sci. Rep.*, 2016, **6**, 20672.
16. C. F. Zhang, L. G. Qiu, F. Ke, Y. J. Zhu, Y. P. Yuan, G. S. Xu, and X. Jiang, *J. Mater. Chem. A*, 2013, **1**, 14329–14334.
17. R. Lv, J. Wang, Y. Zhang, H. Li, L. Yang, S. Liao, W. Gu, and X. Liu, *J. Mater. Chem. A*, 2016, **4**, 15494–15500.
18. T. K. Pal, N. Chatterjee, and P. K. Bharadwaj, *Inorg. Chem.*, 2016, **55**, 1741–1747.
19. X. Y. Guo, F. Zhao, J. J. Liu, Z. L. Liu, and Y. Q. Wang, *J. Mater. Chem. A*, 2017, **5**, 20035–20043.
20. D. K. Singha, S. Bhattacharya, P. Majee, S. K. Mondal, M. Kumar, and P. Mahata, *J. Mater. Chem. A*, 2014, **2**, 20908–20915.
21. H. Sahabudeen, H. Qi, B. A. Glatz, D. Tranca, R. Dong, Y. Hou, T. Zhang, C. Kuttner, T. Lehnert, G. Seifert, U. Kaiser, A. Fery, Z. Zheng and X. Feng, *Nat. Commun.*, 2016, **7**, 1–8.

**Graphical Abstract.**

